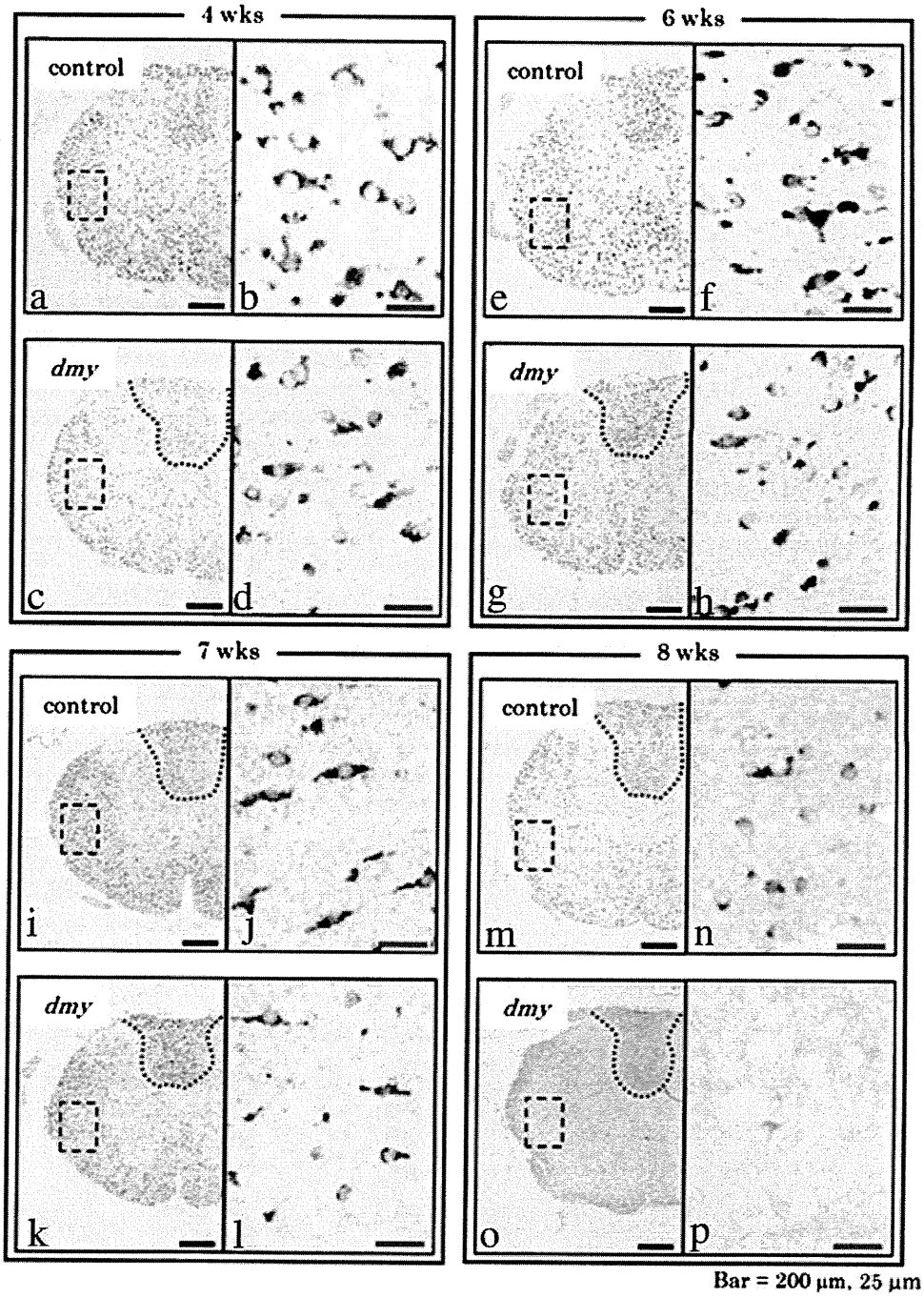

Fig. 2 – In situ hybridization for PLP in the lumbar spinal cord of control (a, b, e, f, i, j, m, n) and *dmy* (c, d, g, h, k, l, o, p) rats. There is no apparent difference between control and *dmy* rats in the morphology of PLP-positive cells until 6 weeks. Marked reduction of PLP-positive cells is found in the lateral funiculus at 8 weeks. The right images are high power views of dot-lined squares of the left images. Black bar, 200 μm; red bar, 25 μm.

(Fig. 3c and d). OLIG2-positive cells were also increased in the ventral funiculus of *dmy* rats (Fig. 4c and d). Immunoreactivity of NG2-positive cells was more conspicuous in the *dmy* rats compared to the control rats at 6 and 7 weeks (Fig. 4a and b). There was no significant difference in the cell density of NG2 in the dorsal funiculus between 6 and 7 weeks.

2.3. *Morphological changes of oligodendrocytes during the development of myelin lesions*

Round to ovoid cells possessing round clear nuclei and abundant light eosinophilic cytoplasm were often found in the white matter of myelin-destructed lesions in the *dmy* rat

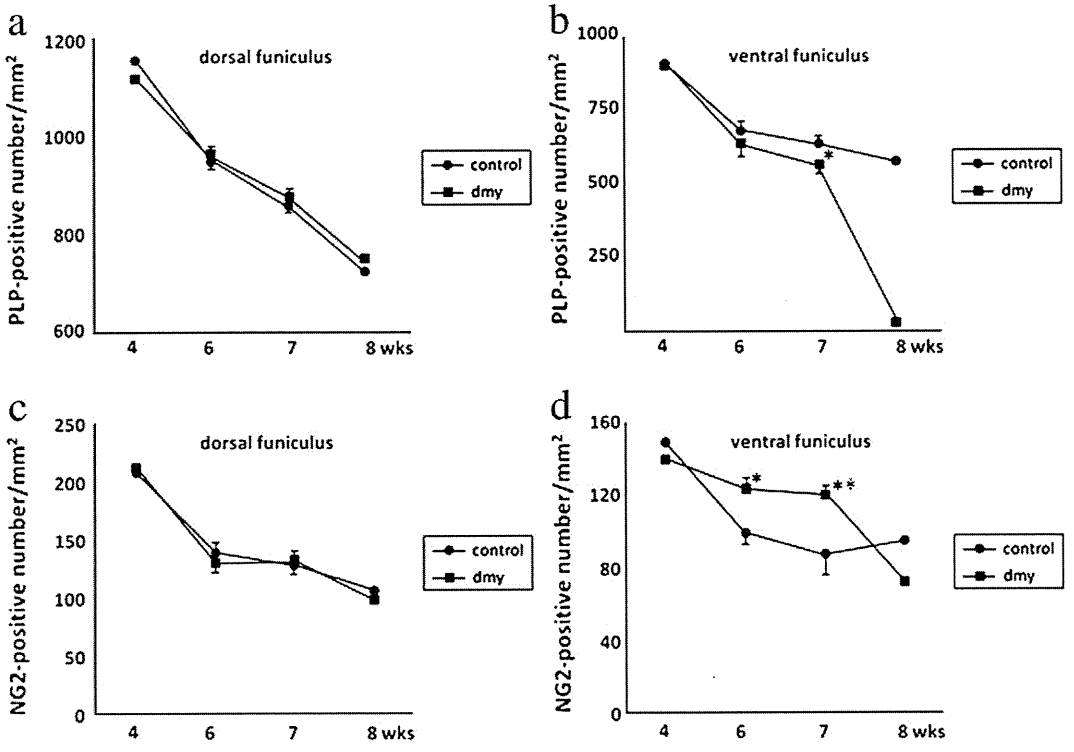

Fig. 3 – The number of PLP-(a, b) and NG2-(c, d) positive cells in the dorsal (a, c) and ventral (b, d) of the spinal cord. There is no difference in cell number between control (circles) and *dmy* (squares) in the dorsal funiculus. At 7 weeks, the cell density of the PLP-positive oligodendrocytes were significantly decreased ($n=3$ in each group) and rapidly decreased at 8 weeks in the ventral funiculus (b). At 6 and 7 weeks, the density of NG2-positive cells in the ventral funiculus of *dmy* rat is significantly increased ($n=3$ in each group) and the density rapidly began to decrease at 8 weeks (d). Presented as the mean ± SD. $^{*}P<0.05$, $^{**}P<0.01$, compared to control rats.

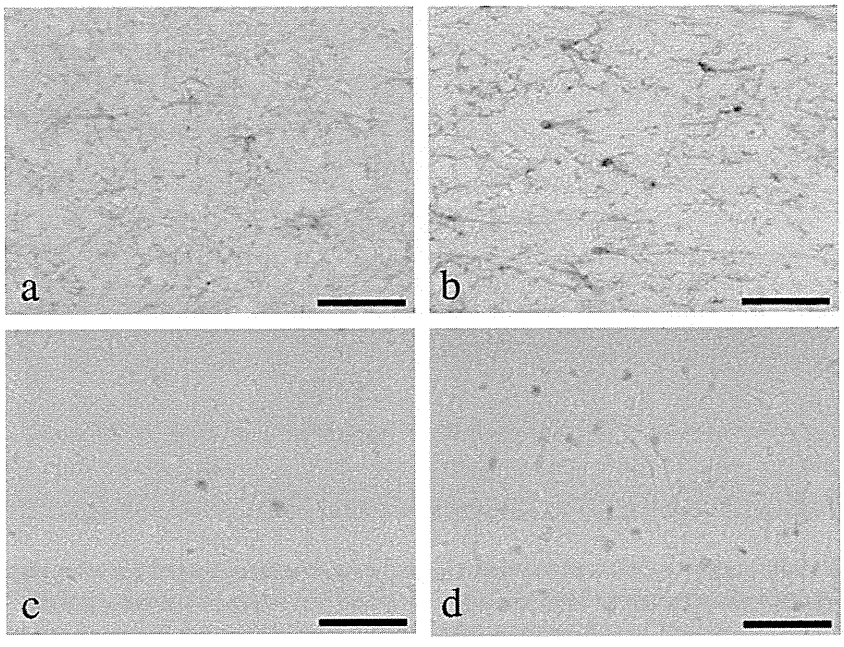

Fig. 4 – NG2 immunohistochemistry in the ventral funiculus of the spinal cord in control (a) and *dmy/dmy* (b) rats aged 7 weeks. Many NG2-positive cells are seen in the *dmy/dmy* rat, compared to the control. NG2-positive cells are intensely stained in *dmy/dmy* rat. Bar, 50 μm. OLIG2 immunohistochemistry in the ventral funiculus of the spinal cord in control (c) and *dmy/dmy* (d) rats aged 7 weeks. Many OLIG2-positive cells are found in the *dmy/dmy* rat compared to the control. Bar, 50 μm.

(Fig. 5a and b). Prohibitin immunohistochemistry revealed that a few positively stained cells were sparsely observed in the white matter of *dmy* rats until 6 weeks and control rats (Fig. 5c), whereas many prohibitin-positive hypertrophic cells were found in the ventral funiculus of *dmy* rats at 7 and 8 weeks (Fig. 5d). These hypertrophic cells were also intensely stained by cytochrome oxidase histochemistry, compared with age-matched control rats (Fig. 5e and f). To identify the origin of hypertrophic cells, serial paraffin sections were stained with prohibitin immunohistochemistry and PLP in situ hybridization. Prohibitin positive hypertrophic cells were expressed PLP mRNA (Fig. 5g and h), indicating that hypertrophic cells are derived from oligodendrocytes.

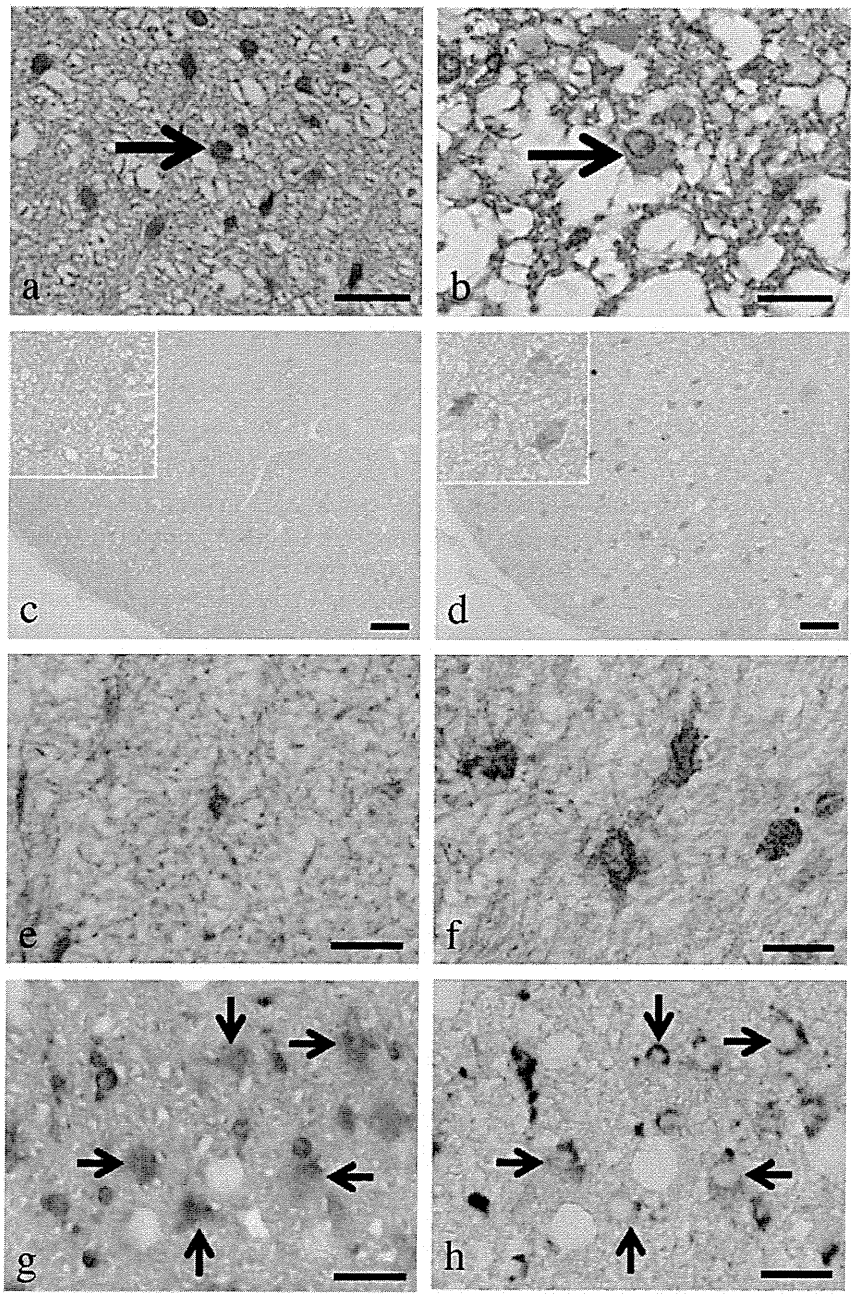

Fig. 5 – Ventral funiculus of the lumbar spinal cord of control (a) and *dmy/dmy* (b) rats aged 8 weeks. Hypertrophic cells with abundant light eosinophilic cytoplasm (arrow) is seen in the *dmy/dmy* rat. Arrow in (a) indicates a possible oligodendrocyte. HE bar, 20 μm. Immunohistochemistry for prohibitin in the lumbar spinal cord of control (c) and *dmy/dmy* (d) rats aged 7 weeks. Insets show higher magnification of the prohibitin-positive cells. Many prohibitin-expressing cells are observed in the *dmy/dmy* rat. Bar, 500 μm. Cytochrome oxidase histochemistry in the ventral funiculus of the lumbar spinal cord of control (e) and *dmy/dmy* (f) rats aged 7 weeks. Intensely stained hypertrophic cells are seen in the *dmy/dmy* rat. Bar, 20 μm. Serially stained sections for prohibitin (g) and PLP in situ hybridization (h). Prohibitin-positive hypertrophic cells are also expressed PLP mRNA. Ventral funiculus of the lumbar spinal cord of 7-week-old *dmy/dmy* rat. Bar, 20 μm.

3. Discussion

Previous electron microscopic and morphometric studies have demonstrated no significant differences in the myelin thickness and fiber size between *dmy* and control rats until the 4th week (Kuwamura et al., 2004). From 5 weeks of age, the myelin thickness in *dmy* rats became significantly less than that of controls, indicating that the progress of myelin destruction during maturation of myelinogenesis and that the *dmy* mutation affect the adequate maintenance of myelin (Kuwamura et al., 2004). The present study reveals that the cell densities and total cell numbers of PLP-positive oligodendrocytes are similar in both *dmy* and control rats until the 6th week but that the number rapidly decreases in the *dmy* rat from 7 weeks of age. In the attractin-deficient *mv* rat, a hypomyelination model, the composition and distribution of major myelin proteins are affected in the spinal cord during postnatal development, whereas the number of oligodendrocytes is not affected. These findings suggest an impairment of oligodendrocyte differentiation and/or a failure of oligodendrocyte to produce myelin proteins in *mv* rats (Izawa et al 2008). Jimpy mouse with a *Plp* mutation exhibits a dysmyelination in the CNS. Jimpy mice produce little CNS myelin, likely due to a premature death of oligodendrocytes throughout the CNS coincident with active myelination (Knapp et al., 1986; Skoff, 1995). Myelin breakdown in the *dmy* rat is considered to be directly related to the loss of myelin-forming oligodendrocytes.

The increased proliferation activity of OPCs was demonstrated by immunohistochemical examination for bromodeoxyuridine (BrdU) and NG2 in the spinal cord of the shiverer mutant (*shi*), which does not form compact myelin due to a deletion in the myelin basic protein gene (Bu et al., 2004). These data suggest that new oligodendrocytes continue to be generated in the dysmyelinated *shi* spinal cord. In a toxin-induced rodent model of demyelination, OPCs increase their expression of Nkx2.2 and Olig2, suggesting that an increased expression of two transcription factors plays an important role in the differentiation of OPCs into remyelinating oligodendrocytes (Fancy et al., 2004). We observed increased NG2+ OPCs in the spinal cord of *dmy* rat compared with the control between the 6th and 7th weeks. This period is consistent with the stage of myelin breakdown in *dmy* rats. Therefore, increased OPCs may try to differentiate into oligodendrocytes and to compensate for the degenerating oligodendrocytes. Nevertheless, myelin collapse develops and the number of OPCs is rapidly decreased at the 8th week.

Positional cloning revealed that the *dmy* rat has a point mutation generating a novel splicing acceptor site in intron 3 of the Mrs2 gene (Kuramoto et al., 2011). Mrs2 encodes an essential component of the major electrophoretic Mg^{2+} influx system in mitochondria of yeast as well as human cells. Our previous electron microscopic study demonstrated the increased number of mitochondria in the cytoplasm of oligodendrocytes in the *dmy* rat. In human mitochondrial disease, increased numbers and abnormal morphology of mitochondria is often observed in the neurons and skeletal muscle, both of which are considered to be a compensatory response to the respiratory dysfunction.

Furthermore, the *dmy* rat has elevated serum lactic acid levels with the progression of the ataxia (Kuramoto et al., 2011). In the present study, we found many oligodendrocytes with abundant cytoplasm that were intensely stained with prohibitin and cytochrome oxidase. This finding reflects the increased number of mitochondria in the oligodendrocytes during the stage of myelin destruction. This increase may be due to the compensation for dysfunction of energy production and suggests that the myelin breakdown in the *dmy* rat is related to the dysfunction of mitochondria in myelin-forming cells. An abnormal iron accumulation and significant upregulation of the antioxidant enzyme heme oxygenase-1 and iron storage protein ferritin has been proved in the *dmy* rat. These findings indicate that iron-mediated oxidative stress is most likely involved in the myelin breakdown of the *dmy* rat and that oligodendrocytes may be primarily affected by the oxidative stress (Izawa et al., 2010). Mice with *Plp*1 duplications (*Plp*1 tg) have major mitochondrial deficits with a 50% reduction in ATP, a drastically reduced mitochondrial membrane potential and increased numbers of mitochondria (Hüttemann et al., 2009). This finding may imply intriguing relation between the myelin formation and energy metabolism in oligodendrocytes.

Mrs2 gene expression in the CNS was more dominantly observed in neurons than oligodendrocytes (Kuramoto et al., 2011). On the other hand, enhanced expression of prohibitin immunohistochemistry was found in the oligodendrocytes, not in the neurons. There is no apparent abnormality in the neurons of *dmy* rats. Myelination requires a complicated interaction between the axons and processes of oligodendrocytes. Thus, the precise pathogenesis of myelin destruction in the *dmy* rat remains to be elucidated.

In conclusion, the *dmy* rat suffers from mitochondrial dysfunction, which results in increased numbers of mitochondria and hypertrophy of oligodendrocytes, leading to myelin destruction. The *dmy* rat may serve as an excellent animal model for studying the relationship between the energy metabolism in oligodendrocytes and the maintenance and/or production of myelin.

4. Experimental procedure

4.1. *Animals*

The original *dmy* rat was discovered in a stock of Sprague–Dawley (SD) rats. The congenic *dmy* rat with a WTC background was established and maintained at Kyoto University in Japan. The WTC.DMY-*dmy* (NBRP#0021) strain was supplied by the National BioResource Project-Rat, Kyoto University (Kyoto, Japan), and used for this study. We mated heterozygous females (*dmy*/+) with heterozygous males (*dmy*/+) and obtained both homozygous and control rats (*dmy*/+ or +/+). The genotypes were evaluated by PCR and restriction enzyme fragmentation pattern of the causative gene, Mrs2 (Kuramoto et al., 2011). Animals were handled according to the Guidelines for Animal Experimentation, Osaka Prefecture University.

4.2. Immunohistochemistry

Rats were deeply anesthetized and perfused transcardially with 4% paraformaldehyde (PFA) in 0.1 M phosphate buffer (PB; pH 7.4) at 4, 6, 7, and 8 weeks of age. Tissue samples from thoracic and lumbar spinal cords were routinely processed and embedded in paraffin. Five-micrometer sections were dewaxed, pretreated in a microwave with citrate buffer (pH 5.0, 10 mM) for 10 min, and incubated in 3% hydrogen peroxide for 10 min. Sections were then incubated overnight at 4 °C with anti-prohibitin mouse monoclonal antibody for mitochondrion (1:1000; AnaSpec) (Coates et al., 2001). After washes in phosphate-buffered saline (PBS), sections were treated with a peroxidase-conjugated anti-mouse IgG antibody (Histofine Simple Stain MAX PO; Nichirei, Japan) for 45 min. Signals were visualized with a 3,3-diaminobenzidine (DAB) substrate kit (Vector Laboratories, USA). Sections were lightly counterstained with hematoxylin.

For the detection of oligodendrocyte precursor cells (OPCs), NG2 and OLIG2 immunohistochemistry was applied for frozen sections. After washing with PBS, the sections were incubated with anti-NG2 rabbit polyclonal (1:1000; Chemicon) or anti-OLIG2 rabbit polyclonal (1:1000; Immuno-Biological Laboratories) antibodies. Horseradish peroxidase-conjugated polymer (Histofine Simple Stain MAX PO; Nichirei, Tokyo, Japan) was used as a secondary antibody. Signals were visualized with a 3,3-diaminobenzidine substrate kit (Vector Laboratories).

4.3. Cytochrome oxidase histochemistry

Frozen spinal cord sections were prepared. Then, 100 μl of freshly prepared reaction buffer [50 mM Tris/HCl (pH 7.4), 0.5 mg/ml diaminobenzidine, 20 μg/ml catalase, and 0.5 mg/ml cytochrome c] was added to each section and slides were incubated for 30 min at 37 °C.

4.4. In situ hybridization for PLP mRNA

For riboprobe preparation, a 568 bp fragment of the rat PLP cDNA (GenBank accession no. NM_0309906539) was amplified by PCR (forward primer, 5′-TTT GGA GTG GCA CTG TTC TG-3′, nucleotide position 201–220; reverse primer, 5′-GAA AAG CAT TCC ATG GGA GA-3′, nucleotide position 749–768). The PCR product was subcloned into pGEM T-Easy Vector (Promega, USA). Digoxigenin (DIG)-labeled sense or antisense riboprobe was synthesized with SP6 or T7 RNA polymerase (Roche, Switzerland), respectively. For in situ hybridization, lumbar spinal cords were fixed in 4% PFA in 0.1 M PB at 4 °C overnight, treated with 30% sucrose in PBS at 4 °C for 2 or 3 days, and frozen at −80 °C. Ten-micrometer transverse sections were cut on a cryostat. The in situ hybridization procedure was carried out as reported (Sim et al., 2002). Before hybridization, sections were pretreated as follows: 1) 4% PFA in PBS for 15 min, 2) 10 μg/ml proteinase K (Invitrogen, USA) at 37 °C for 12 min, 3) 0.2 M HCl for 10 min, 4) 0.25% acetic anhydride in 0.2 M triethanolamine (pH 8.0) for 10 min. DIG-labeled riboprobes were diluted in hybridization buffer (50% formamide, 10 mM Tris–HCl, pH 8.0, 200 μg/ml yeast tRNA, 10% dextran sulfate, 1× Denhardt's solution, 600 mM NaCl, 0.25% SDS, 1 mM EDTA) and were placed on each slide. Sections were then coverslipped and incubated at 65 °C for 16 h. After hybridization, sections were rinsed in 2× sodium saline citrate (SSC) containing 50% formamide at 65 °C for 30 min, treated with 20 μg/ml RNase A (Roche) at 37 °C for 30 min, and rinsed in 2×, 0.2×, and 0.1× SSC (each at 65 °C for 20 min). RNA hybrids were immunostained with alkaline phosphatase-conjugated anti-DIG antibody (1:1000; Roche) at 4 °C overnight and were visualized with BCIP/NBT substrate (Roche).

4.5. Image analysis

Tissue sections were captured with a light microscope (BX41; Olympus, Japan) and a digital camera (DS-Fi1; Nikon, Japan). Transverse spinal cord sections for NG2 immunohistochemistry and PLP in situ hybridization were collected from three different animals in each experimental group. The positive cells were counted in the dorsal and lateral funiculus using image-analyzing software (WinRoof; Mitani Corporation, Japan).

4.6. Cell counts

Three different transverse sections from three different animals were evaluated at 6 and 7 weeks of age. The data are presented as the number of NG2- and PLP-positive cells per square millimeters.

4.7. Statistical analysis

Data are presented as the means±standard deviation. Statistical analysis was performed using one-way analysis of variance followed by Tukey's test. A value of P less than 0.05 was considered statistically significant.

Acknowledgments

We are thankful to the National BioResource Project-Rat (http:///www.anim.med.kyoto-u.ac.jp/NBR/) in Japan for providing WTC.DMY-*dmy* (NBRP#0021) rat strain. This work was supported by Grant-in-Aid for Scientific Research from Japan Society for Promotion of Science (JSPS; no. 20580341).

Appendix A. Supplementary data

Supplementary data to this article can be found online at doi:10.1016/j.brainres.2011.03.009.

REFERENCES

Al-Saktawi, K., McLaughlin, M., Klugmann, M., Barrie, S.J., McCulloch, M.C., Montague, P., Kirkham, D., Nave, K.A., Griffiths, I.R., 2003. Genetic background determines phenotypic severity of the Plp rumpshaker mutation. J. Neurosci. Res. 72, 12–24.

Bu, J., Banki, A., Wu, Q., Nishiyama, A., 2004. Increased NG2+ glial cell proliferation and oligodendrocyte generation in the hypomyelinating mutant shiverer. Glia 48, 51–63.

Coates, P.J., Nenutil, R., McGregor, A., Picksley, S.M., Crouch, D.H., Hall, P.A., Wright, E.G., 2001. Mammalian prohibitin proteins respond to mitochondrial stress and decrease during cellular senescence. Exp. Cell Res. 265, 262–273.

Duncan, I.D., Lunn, K.F., Holmgren, B., Urba-Holmgren, R., Brignolo-Holmes, L., 1992. The taiep rat: a myelin mutant with an associated oligodendrocyte microtubular defect. J. Neurocytol. 21, 870–884.

Fancy, S.P., Zhao, C., Franklin, R.J.M., 2004. Increased expression of Nkx2.2 and Olig2 identifies reactive oligodendrocyte progenitor cells responding to demyelination in the adult CNS. Mol. Cell. Neurosci. 27, 247–254.

Griffiths, I.R., 1996. Myelin mutants: model systems for the study of normal and abnormal myelination. BioEssays 18, 789–797.

Hüttemann, M., Zhang, Z., Wullins, C., Bessert, D., Lee, I., Nave, K.A., Appikatla, S., Skoff, R.P., 2009. Different proteolipid protein mutants exhibit unique metabolic defects. ASN Neuro. 1, 165–180.

Izawa, T., Takenaka, S., Ihara, H., Kotani, T., Yamate, J., Franklin, R.J.M., Kuwamura, M., 2008. Cellular responses in the spinal cor during development of hypomyelination in the mv rat. Brain Res. 1195, 120–129.

Izawa, T., Yamate, J., Franklin, R.J.M., Kuwamura, M., 2010. Abnormal iron accumulation is involved in the pathogenesis of the demyelinating dmy rat but nor in the hypomyelinating mv rat. Brain Res. 1349, 105–114.

Kitada, M., Rowitch, D.H., 2006. Transcription factor co-expression patterns indicate heterogeneity of oligodendroglial subpopulations in adult spinal cord. Glia 54, 35–46.

Knapp, P.E., Skoff, R.P., Redstone, D.W., 1986. Oligodendroglial cell death in jimpy mice: an explanation for the myelin deficit. J. Neurosci. 6, 2813-1822.

Knapp, P.E., Adjan, V.V., Hauser, K.F., 2009. Cell-specific loss of k-opioid receptors in oligodendrocytes of the dysmyelinating jimpy mouse. Neurosci. Lett. 451, 114–118.

Kuramoto, T., Sotelo, C., Yokoi, N., Serikawa, T., Gonalons Sintes, E., Canto Martorell, J., Guenet, J.L., 1996. A rat mutation producing demyelination (dmy) maps to chromosome 17. Mamm Geneome 7, 890–894.

Kuramoto, T., Kuwamura, M., Tokuda, S., Izawa, T., Nakane, Y., Kitada, K., Akao, M., Guenet, J.L., Serikawa, T., 2011. A mutation in the gene encoding ion channel mediating influx of Mg^{2+} into mitochondria results in demyelination in the rat. PLoS Genet. 7, e1001262.

Kuwamura, M., Kanehara, T., Tokuda, S., Kumagai, D., Yamate, J., Kotani, T., Nakane, Y., Kuramoto, T., Serikawa, T., 2004. Immunohistochemical and morphometrical studies on myelin breakdown in the demyelination (dmy) mutant rat. Brain Res. 1022, 110–116.

Kwiecien, J.M., O'Connor, L.T., Goetz, B.D., Delaney, K.H., Fletch, A.L., Duncan, I.D., 1998. Morphological and morphometric studies of the dysmyelinating mutant, the Long Evans shaker rat. J. Neurocytol. 27, 581–591.

Sim, F.J., Zhao, C., Penderis, J., Franklin, R.J.M., 2002. The age-related decrease in CNS remyelination efficiency is attributable to an impairment of both oligodendrocyte progenitor recruitment and differentiation. J. Neurosci. 22, 2451–2459.

Skoff, R.P., 1995. Programmed cell death in the dysmyelinating mutants. Brain Pathol. 5, 283–288.

Song, J., Ocnnor, L.T., Yu, W., Baas, P.W., Duncan, I.D., 1999. Microtubule alterations in cultured taiep rat oligodendrocytes lead to deficits in myelin membrane formation. J. Neurocytol. 28, 671–683.

Received Date : 24-Nov-2011
Revised Date : 27-Mar-2012
Accepted Date : 04-Apr-2012
Article type : Original Article

Impairment of fear-conditioning responses and changes of brain neurotrophic factors in diet-induced obese mice

Short title: Cognition and brain neurotrophins in diet-induced obese mice (53/60)

Nobuko Yamada-Goto [a], Goro Katsuura [a], Yukari Ochi [a], Ken Ebihara [a, b], Toru Kusakabe [a], Kiminori Hosoda [a], Kazuwa Nakao [a]

[a] Department of Medicine and Clinical Science, Kyoto University Graduate School of Medicine, 54, Shougoin Kawahara-cho, Sakyo-ku, Kyoto 606-8507, Japan.

[b] Department of Experimental Therapeutics, Translational Research Center, Kyoto University Hospital, 54, Shougoin Kawahara-cho, Sakyo-ku, Kyoto 606-8507, Japan.

Correspondence to Goro Katsuura, PhD

Department of Medicine and Clinical Science, Kyoto University Graduate School of Medicine, 54, Shougoin Kawahara-cho, Sakyo-ku, Kyoto 606-8507, Japan.

Phone: +81-75-751-3171

Fax: +81-75-771-9452

E-mail address: goro@kuhp.kyoto-u.ac.jp

Abstract

Recent epidemiological studies demonstrate that obesity is related to high incidence of cognitive impairment. In the present study, cognitive behaviors in diet-induced obese (DIO) mice fed 60% high-fat diet for 16 weeks were compared with those in mice fed control diet (CD) in fear-conditioning tests including both contextual and cued elements which preferentially depend on the amygdala and hippocampus, respectively, and moreover, the contents of brain-derived neurotrophic factor (BDNF) and neurotrophin-3 (NT-3) in the brain areas were examined in both CD and DIO mice. In fear-conditioning tests, the freezing percentage of both contextual fear and cued fear responses in DIO mice were significantly lower than in CD mice. The contents of BDNF in the cerebral cortex and hippocampus of DIO mice were significantly lower than those of CD mice. Its receptor, full-length TrkB in the amygdala of DIO mice significantly decreased compared with that of CD mice, but not in the cerebral cortex, hippocampus and hypothalamus. On the other hand, the contents of NT-3 in the hippocampus, amygdala and hypothalamus of DIO mice were significantly higher than those of CD mice. Its receptor, full-length TrkC was not significantly different between CD and DIO mice. The present study demonstrated that DIO mice show impairment of both amygdala-dependent contextual and hippocampus-dependent cued responses in the fear-conditioning tests, and imbalance in the interaction between the BDNF and NT-3 systems in the cerebral cortex, hippocampus and amygdala related to cognition and fear.

Keywords:

high-fat diet, obese mouse, fear-conditioning test, cognition, brain neurotrophic factors.

Introduction

Obesity is defined as increased adipose mass resulting from chronic excess of energy intake over energy expenditure. Obesity is becoming a world-wide problem as it is associated with serious comorbidities, including a high incidence of type II diabetes and cardiovascular disease, and increased risk of many forms of cancer. In addition, epidemiological studies have demonstrated that the incidence of depression and cognitive impairment is higher in obese subjects than normal body weight subjects (1, 2). We recently demonstrated that impaired leptin action in the hippocampus is involved in depression associated with diet-induced obesity in mice (3).

Energy homeostasis including food intake and energy consumption has been demonstrated to be regulated predominantly by orexigenic and anorexigenic systems in the hypothalamus. Recently, several lines of evidence have indicated that energy regulations are also modulated by extra-hypothalamic brain areas originally related to regulation of emotion and cognition, such as the nucleus accumbens, amygdala, hippocampus and cerebral cortex (4). These findings suggest that maintaining energy homeostasis and regulating emotion and cognition share common brain regions, as well as bidirectional interaction between energy regulation and emotional/cognitive functions. In this regard, obese rats fed saturated fat and refined sugar show impaired acquisition and retention of spatial memory in the water maze test which is dependent on the

hippocampus (5). Electrophysiological studies in genetically obese Zucker rats with leptin-receptor deficiency demonstrated that long-term potentiation (LTP) of the hippocampal CA1 region, which is closely related to memory formation and is predominately regulated by the glutamatergic system, especially N-methyl-D-aspartate (NMDA) receptors and α-amino-3-hydroxyl-4-isoxazolepropionic acid (AMPA) receptors (6), is markedly impaired in comparison with lean rats (7). These findings suggest dysfunction of the hippocampus in obese animals. The amygdala, as well as the hippocampus, which has been established as playing a pivotal role in regulation of fear, emotion and cognition (8, 9), has been suggested to be involved in energy regulation because lesion of the amygdala has been reported to induce hyperphagia, resulting in marked obesity (10, 11). Moreover, the amygdala has recently been demonstrated to be one of the brain regions regulating appetite via activation of the melanocortin system (12).

Memory formation involves long-term structural alterations of synapses, so-called neuronal plasticity involving cellular and molecular mechanisms of synapse formation, neurite outgrowth, and behavioral adaptation (13). Cellular and molecular events involved with neuronal plasticity are under the range of action of neurotrophic factors including brain-derived neurotrophic factor (BDNF) and neurotrophin-3 (NT-3) (14, 15). BDNF and NT-3 act via high-affinity tyrosine kinase receptors, TrkB and TrkC, respectively (16, 17). The BDNF system in the brain is demonstrated to have anti-obesity and anti-diabetic effects, as well as regulation of neural modeling and cognitive processes (18, 19, 20, 21). Although actions of NT-3 in the brain on energy regulation are not yet known, BDNF and NT-3 act in opposite directions in neurite outgrowth and neural activities (22, 23). Moreover, glucocorticoid is reported to show

opposite effect on regulation of BDNF and NT-3 expressions in the brain (24).

To explore cognition in diet-induced obese (DIO) mice, in the present study we examined the cognitive behavior of DIO mice fed high-fat diet (HFD) using fear-conditioning tests involving regulation mainly by the hippocampus and amygdala (25), and also investigated the contents of BDNF and NT-3 and the expressions of their receptors, TrkB and TrkC in the cerebral cortex, hippocampus, amygdala and hypothalamus of DIO mice as compared with control mice.

Materials and Methods

Animals and diets

Male C57BL/6J mice (6 weeks old) were obtained from Japan SLC, Inc. (Shizuoka, Japan). They were housed on a 12:12-h light-dark cycle (the light was switched on at 7:00 am) and at 23 ± 1°C room temperature. The animals had ad libitum access to water and food. They were randomly divided into two groups: mice fed HFD (DIO: Research Diets, Inc., New Brunswick, NJ; No. D12492: 524 kcal per 100 g) and mice fed control diet (CD: CE-2, CLEA Japan, Inc., Tokyo, Japan: 346.8 kcal per 100 g). Both groups were fed for 16 weeks. Experiments were performed between 13:00 and 15:00. All experiments were performed in accordance with the guidelines established by the Institutional Animal Investigation Committee at Kyoto University and the United States National Institutes of Health Guide for the Care and Use of Laboratory Animals. Every effort was made to optimize the comfort and minimize the use of animals.

Blood sampling and analysis of metabolic parameters

Blood samples were taken from the thoracic aorta using a syringe containing heparin sodium and aprotinin. The blood samples were centrifuged at 14,000 rpm for 2 min, and plasma was separated and stored at -20°C until assayed. Plasma metabolic parameters were analyzed according to our previous report (3).

Fear-conditioning test

The fear-conditioning test was performed as described in a previous report (26). Briefly, training sessions consisted of pairing a neutral stimulus (conditioned stimulus; CS) of a tone and an aversive stimulus (unconditioned stimulus; US) of an electric foot shock. The conditioning chamber was surrounded by a sound-attenuated chest with an observation window. The foot shock was delivered via the grid floor composed of stainless steel rods. The tone was provided by a ventilation fan making a noise of 65 dB. On the first day, each mouse was trained 10 times to associate foot shock with the tone, which was presented for 30 s as a conditioned stimulus and 0.5 mA foot shock for 2 s as an unconditioned stimulus. Mice were then returned to their home cages. Twenty-four hours later, the contextual response and the cued response were observed. To examine the contextual conditioning response, each mouse was placed in the conditioning chamber without the tone for 5 min and freezing behavior was measured every 1 min. Freezing was defined as the absence of all movement except for respiration. Freezing was monitored continuously by an observer and was recorded on a chart via a switch. Freezing time was summed, and the freezing percentage was calculated per minute. This response mainly depends on the hippocampus. Three hours after termination of the

contextual conditioning response, the cued conditioning response was examined by placing each mouse in a new clear plastic cage with the tone for 3 min. Freezing behavior was measured every 1 min. This response mainly depends on the amygdala.

Jumping-vocalization response

To compare the responses to foot shock of DIO mice with those of CD mice, the test was performed as described in a previous report (26) with the foot shock box used in the experiment on contextual fear conditioning of CD and DIO mice. Each mouse was placed individually in the box. After a 3-min period of habituation to the test box, shock titrations were continued upwards and downwards in a stepwise manner (0.5 mA, 2 s). Jumping responses to the foot shock were scored as 0 - 3 and vocalization responses to the foot shock were scored as 0 - 3. Response scores 0, 1, 2 and 3 indicate no response, slight response, moderate response and marked response, respectively. Data are presented as the total score of these two responses.

Spontaneous locomotor activity

As described in our previous report (3), spontaneous locomotor activity was measured for 30 min immediately after CD and DIO mice fed CD and HFD, respectively, for 16 weeks were placed in a new cage.

Elevated plus-maze test

This test was performed according to our previous report (27). The elevated plus-maze (Muromachi Kikai Co., Ltd., Tokyo, Japan) was constructed of gray Plexiglas and consisted of four arms (300 mm long × 60 mm wide): two closed arms with high gray

walls (150 mm high) and two open arms with a small raised lip (3 mm). The maze was elevated to a height of 400 mm above the ground. At least 1 hr before the test, mice were transferred to a standby room (20 lx) that was separated from the test room. Experiments were performed between 13:00 and 15:00. Each mouse was placed on the center platform facing an open arm to initiate the test session. Mice were allowed to freely explore the apparatus under overhead fluorescent lighting (20 lx) for 5 min. Increased exploration of the relatively open arms is indicative of reduced anxiety-like behavior in this paradigm. Open/closed arm entries and time spent in the open/closed arms were scored. Arm entries were scored upon entry of the two front paws into the arm.

Measurement of BDNF and NT-3 contents in the brain

BDNF and NT-3 contents in the brain of CD and DIO mice fed CD and HFD, respectively, for 16 weeks were measured according to our previous report (3) using commercially available measurement kits for BDNF (BDNF Emax® ImmunoAssay System: Promega Inc., Madison, WI) and for NT-3 (NT-3 Emax® ImmunoAssay System: Promega Inc., Madison, WI).

Western blot analysis of TrkB and TrkC

Western blotting of full- length TrkB and TrkC in the brain of CD and HFD mice was performed according to our previous report (3). Full-length TrkB and TrkC were detected using rabbit polyclonal anti-TrkB antibody (sc-8316, Santa Cruz Biotechnology, Inc., Santa Cruz, CA) and rabbit polyclonal anti-TrkC antibody (sc-14025, Santa Cruz Biotechnology, Inc.), respectively. Results represent the

densitometry data relative to glyceraldehyde-3-phosphate dehydrogenase (GAPDH) detected in each sample.

Data analysis

All values are given as the mean ± SEM. Statistical analysis of the data was carried out by analysis of variance (ANOVA) followed by Dunnett's multiple-range test. Statistical significance was defined as $p < 0.05$.

Results

Metabolic parameters in CD and DIO mice

The metabolic parameters in CD and DIO mice are shown in Table 1. The body weight of DIO mice was 1.6 times greater than that of CD mice. Plasma levels of glucose, insulin and leptin in DIO mice were significantly high compared with those in CD mice.

Fear-conditioning response

CD mice exhibited 93% freezing due to fear in the 1st session in the contextual conditioning response, and the freezing percentage gradually decreased during the sessions to reach 60% in the 5th session (Fig. 1). In DIO mice, the freezing percentage of the contextual fear response was significantly lower than that in CD mice in each session (Fig. 1). DIO mice exhibited 64% freezing percentage in the 1st session of the contextual fear response, and the freezing percentage subsequently decreased during the sessions to 23% in the 5th session (Fig. 1). Similarly, the freezing percentage of the cued fear response in DIO mice was 47% in the first session which was much lower

than the 81% in CD mice, and a significant decrease in freezing percentage of DIO mice was observed over the course of three cued sessions compared with CD mice (Fig. 1).

Jumping-vocalization test, spontaneous locomotor activity and elevated plus-maze test

To compare the sensitivities to foot shock between CD and DIO mice, the jumping-vocalization test was used. No difference in scores of jumping-vocalization test was found between CD (score: 3.2 ± 0.3; n=14) and DIO (score: 2.6 ± 0.1; n=14) mice. To explore the involvement of motor activity and anxiety in impaired fear-conditioning responses in DIO mice, spontaneous locomotor activity for 30 min following placement of mice into new cages and behaviors in the elevated plus-maze test were examined. Spontaneous locomotor activity was not different between CD and DIO mice after 16-week feeding of each diet (data not shown). Moreover, both entry times and time spent in the dark and light arms in the elevated plus-maze test were not different between CD and DIO mice (data not shown).

BDNF and NT-3 contents in the brain areas

BDNF contents in the cerebral cortex and hippocampus of DIO mice had significantly decreased to approximately 70% and 60% of CD mice, respectively (Fig. 2A). BDNF contents in the amygdala and hypothalamus of DIO mice also tended to decrease compared with those of CD mice (Fig. 2A). In contrast to the changes of BDNF contents, NT-3 contents in the hippocampus, amygdala and hypothalamus of DIO mice significantly increased to 150%, 165% and 230% of those of CD mice, respectively (Fig. 2B). NT-3 contents in the cerebral cortex also tended to be higher than those of CD mice

(Fig. 2B).

Expression of full-length TrkB and TrkC receptors in the brain areas

The expression of full-length TrkB in the amygdala of DIO mice significantly decreased to approximately 70% of CD mice, but not in the cerebral cortex, hippocampus and hypothalamus (Fig. 3A). The full-length TrkC expressions in four brain areas were not significantly different between CD and DIO mice (Fig. 3B).

Discussion

The present study demonstrated that DIO mice showed significant reduction of both hippocampus-dependent contextual and amygdala-dependent cued fear responses of fear-conditioning test. However, the response to electric foot shock, locomotor activity and anxiety-like behavior of DIO mice were the same as those of CD mice. Interestingly, BDNF contents in the cerebral cortex and hippocampus of DIO mice were significantly lower than those of CD mice, while NT-3 contents in the hippocampus, amygdala and hypothalamus of DIO mice were significantly higher than those of CD mice. The expression of full-length TrkB for BDNF in the amygdala of DIO mice significantly decreased compared that of CD mice, while the expressions of full-length TrkC for NT-3 in the brain regions were not different between CD and DIO mice. These findings demonstrated that DIO mice display impaired cognition in the fear-conditioning test with imbalanced interaction between BDNF and NT-3 systems in the cerebral cortex, hippocampus and amygdala related to cognition and fear.

Chronic dietary fat intake, especially saturated fatty acid intake, is reported to

contribute to deficits of hippocampus-dependent spatial cognition in the water maze test of rats (5, 6, 28). The adverse effects of high-dense diets on learning and memory have been associated with impaired hippocampal synaptic plasticity and suppressed neurogenesis (29, 30, 31).

Long-term structural alterations of synapses, so-called neuronal plasticity, are regulated by several synaptic molecules including neurotrophic factors, such as BDNF (15), and have been demonstrated to be essential for spatial learning performance which is dependent primarily on hippocampal functions (32). Animals lacking BDNF show deficits in LTP related to processes of learning and memory, and in hippocampus-dependent spatial learning, which can be amended by exogenous BDNF (32). Although the mechanisms by which a high-fat diet can affect BDNF expression are largely unknown, in the present study the feeding of high-fat diet or obesity led to reduction of BDNF contents in the hippocampus and cerebral cortex to the extent that cognitive performance was compromised. In contrast to the decrease in BDNF contents, the present study demonstrated that NT-3 contents were significantly increased in the hippocampus, amygdala and hypothalamus of DIO mice compared with those of CD mice. BDNF and NT-3 oppose one another in regulating the dendritic growth of pyramidal neurons in the hippocampus and neural activity (22, 23). NT-3 was reported to inhibit the dendritic growth stimulated by BDNF (22). The amygdala, which is well established to play a pivotal role in regulation of fear, emotion and cognition (8, 9), is suggested to be involved in energy regulation because lesion of the amygdala has been reported to induce hyperphasia, resulting in marked obesity (10, 11). Moreover, the amygdala has recently been demonstrated to be one of the brain regions regulating appetite via activation of the melanocortin system (12). Taken together, these findings

suggest that the impaired fear-conditioning response in DIO mice is attributed to the decrease of BDNF which facilitates memory processes and the antagonistic actions of NT-3 against BDNF in the hippocampus and amygdala, while the present study did not address the mechanisms of the changes in BDNF and NT-3 contents in the brain of DIO mice.

Several lines of electrophysiological and behavioral evidence demonstrate that leptin and insulin enhance hippocampal synaptic plasticity and improve learning and memory (31, 33). Electrophysiological studies in genetically obese Zucker rats with leptin-receptor deficiency demonstrated that LTP of the hippocampal CA1 region, which is closely related to learning and the formation of memory and is regulated by NMDA and AMPA receptors (6), is markedly impaired in comparison with lean rats (7). Streptozotocin-treated insulin-deficient rats are reported to exhibit impaired cognition in the water maze test which is dependent on the hippocampus (34). Therefore, it seems likely that impairment of actions of leptin or insulin might be attributable to cognitive deficits in obesity and diabetes mellitus (35, 36). Although there is no direct evidence for the impairment of cognition in DIO mice, the impaired cognitive behaviors of fear-conditioning tests observed in this study may be, in part, mediated by decreased inherent functions of leptin and insulin in the brain in spite of high plasma levels of leptin and insulin, so-called leptin resistance or insulin resistance associated with obesity.

The present study has shown that DIO mice exhibit impairment of both hippocampus-dependent contextual and amygdala-dependent cued responses of the fear-conditioning test. Moreover, BDNF contents in the hippocampus and cerebral cortex and of DIO mice, while NT-3 contents increase in the hippocampus, amygdala

and hypothalamus of DIO mice, in comparison to CD mice. The expression of TrkB in the amygdala of DIO mice decreases compared with CD mice. These findings suggest that high-fat diet consumption may contribute to aspects of dysfunction in the central nervous system.

Acknowledgments

This work was supported in part by research grants from the Ministry of Education, Culture, Sports, Science and Technology of Japan and the Ministry of Health, Labour and Welfare of Japan.

Conflict of interest

The authors declared no conflict of interest.

References

1. Elias MF, Elias PK, Sullivan LM, Wolf PA, D'Agostino RB. Lower cognitive function in the presence of obesity and hypertension: the Framingham heart study. Int J Obes 2003; 27: 260-268.
2. Whitmer RA, Gunderson EP, Barrett-Connor E, Quesenberry CP Jr, Yaffe K. Obesity in middle age and future risk of dementia: a 27 year longitudinal population based study. BMJ 2005; 330: 1360-1364.
3. Yamada N, Katsuura G, Ebihara K, Kusakabe T, Hosoda K, Nakao K. Impaired CNS leptin action is implicated in depression associated with obesity. Endocrinology 2011; 152: 2634-2643.
4. Morton GJ, Cummings DE, Baskin DG, Barsh GS, Schwartz MW. Central nervous system control of food intake and body weight. Nature 2006; 443: 289-295.